JACS
JOURNAL OF THE AMERICAN CHEMICAL SOCIETY
Communication
pubs.acs.org/JACS

Enhancing Proton Conduction in 2D Co–La Coordination Frameworks by Solid-State Phase Transition

Song-Song Bao,[†] Kazuya Otsubo,[‡] Jared M. Taylor,[‡] Zheng Jiang,[§] Li-Min Zheng,*[,†] and Hiroshi Kitagawa*[,‡]

[†]State Key Laboratory of Coordination Chemistry, Coordination Chemistry Institute, School of Chemistry and Chemical Engineering, Nanjing University, Nanjing 210093, P. R. China

[‡]Division of Chemistry, Graduate School of Science, Kyoto University, Kitashirakawa-Oiwakecho, Sakyo-ku, Kyoto 606-8502, Japan

[§]Shanghai Institute of Applied Physics, Shanghai Synchrotron Radiation Facility, Chinese Academia Science, Shanghai 201204, P. R. China

Supporting Information

ABSTRACT: We report that a new 2D 3d–4f phosphonate $[Co^{III}La^{III}(notpH)(H_2O)_6]ClO_4{\cdot}5H_2O$ (**CoLa-II**) can undergo a phase transition above 45 °C and 93% relative humidity, resulting in $[H_3O][CoLa(notp)(H_2O)_4]ClO_4{\cdot}3H_2O$ (**CoLa-III**). The transition is accompanied by the release of the proton from intralayer to interlayer, and thus the proton conductivity of the material is increased by 1 order of magnitude.

Proton-conducting materials are essential components of fuel cells.[1] The high proton conductivity and wide operating temperature are two top issues for application of these materials. To obtain the high-performance proton conductors, it is important to realize the relation between structure and properties, which gives insight into the proton-conduction pathway and mechanism. Recently, metal–organic frameworks (MOFs) or porous coordination polymers (PCPs) attract much attention as they show precise structures that can be designed and constructed, high proton conductivities, and wide operating temperatures.[2−6] Many attempts have been made in order to enhance the proton conductivities of these materials under humid conditions. One is to increase the hydrophilicity of the channels, which could host more proton carrier molecules and ions.[7] Another approach is to increase the acidity of the channels by introducing acid groups into the hydrophilic channels.[8,9] The coordinated water molecules as components of media are also favorable because their acidity is enhanced by the metal cations.[10] Herein we propose a new approach to enhance the proton conductivity, e.g., an *in situ* solid-state phase transition approach which involves the release of the proton from intralayer to interlayer space.

Our strategy is to use a metallo-ligand $Co^{III}(notpH_3)$ $[C_9H_{18}N_3(PO_3H_2)_3$, $notpH_6]$ to react with lanthanide ion to build a new 3d–4f layered phosphonate compound $[CoLa(notpH)(H_2O)_6]ClO_4{\cdot}5H_2O$ (**CoLa-II**). This compound contains acidic phosphonate groups and coordinated water molecules within the layer and lattice water molecules between the layers, hence resulting in hydrophilic interlayer channels as efficient proton conducting pathways.[11] More interestingly, it experiences a solid-state phase transition above 45 °C and 93% relative humidity (RH), leading to a new phase $[H_3O][CoLa(notp)(H_2O)_4]ClO_4{\cdot}3H_2O$ (**CoLa-III**). The release of proton from intralayer phosphonate group into the interlayer space can significantly enhance the proton conductivity of the material by 1 order of magnitude. The proton conductivity of $[CoLa(notp)(H_2O)_4]{\cdot}8H_2O$ (**CoLa-I**),[12] reported previously by us, is also investigated for comparison.

Compound **CoLa-II** is prepared by the reaction of $Co(notpH_3)$ and $La(ClO_4)_3$ in a 1:1 molar ratio in the aqueous solution, with the pH adjusted to ∼0.8 by $HClO_4$. Single crystal structural analysis reveals that **CoLa-II** crystallizes in monoclinic $P2_1/n$ space group.[13] The asymmetric unit contains one Co^{3+}, one La^{3+}, one $notpH^{5-}$, one ClO_4^-, six coordinated and five lattice water molecules (Figure S1). The Co atom has a distorted octahedral geometry, surrounded by three N and three O from the same $notpH^{5-}$ ligand. The $[Co(notpH)]^{2-}$ behaves as a tridentate metallo-ligand and links to three La^{3+} ions by phosphonate oxygen atoms O(2), O(5), and O(8). Each La is nine-coordinated with three sites provided by phosphonate oxygen atoms and the remaining six by water molecules. The $\{CoN_3O_3\}$ and $\{LaO_9\}$ polyhedra are each corner-shared with the $\{PO_3C\}$ tetrahedra, forming a positively charged waved layer containing 24-membered rings made up of three Co, three La, six P, and 12 O atoms (Figure 1a, right). The ClO_4^- anions and lattice water molecules fill in the interlayer space with extensive hydrogen-bond interactions (Figure 1b, right). The interlayer distance is 15.94 Å.

The structure of **CoLa-II** is closely related to that of **CoLa-I**,[12] where the $Co(notp)^{3-}$ mononuclear species are connected by La^{3+} ions into a waved layer. The main difference includes: (1) The layer is neutral in **CoLa-I** while positive in **CoLa-II** due to the protonation of one phosphonate oxygen; (2) each $Co(notp)^{3-}$ is linked to four La^{3+} in **CoLa-I**, while each $Co(notpH)^{2-}$ is connected to three La^{3+} in **CoLa-II**, thus leading to layers containing 12- and 16-member rings in the former and 24-member rings in the latter (Figure 1a); and (3) the La^{3+} is eight-coordinated by four phosphonate oxygen and four water molecules in **CoLa-I**, while nine-coordinated by three phosphonate oxygen and six water molecules in **CoLa-II**

Received: June 13, 2014
Published: June 19, 2014

dx.doi.org/10.1021/ja505916c | J. Am. Chem. Soc. 2014, 136, 9292–9295

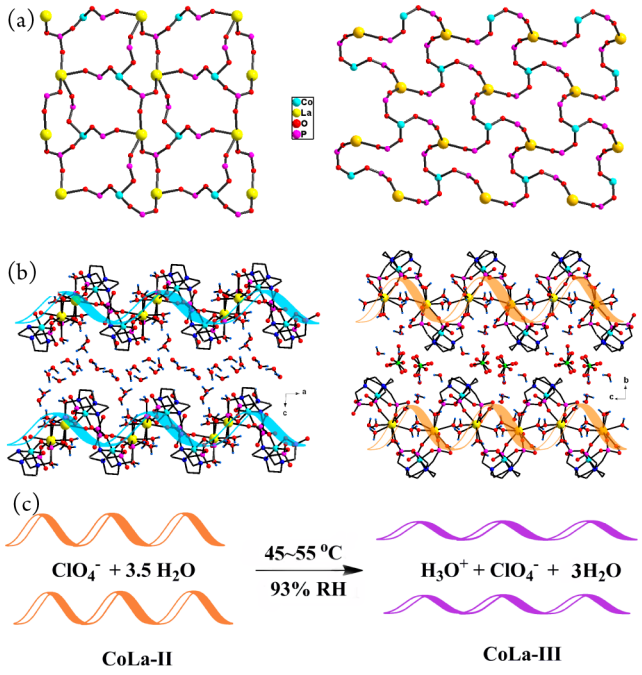

Figure 1. (a) Single layer in structures **CoLa-I** (left) and **CoLa-II** (right). All C and H atoms as well as the coordinated water molecules are omitted for clarity. (b) Packing diagrams of structures **CoLa-I** (left) and **CoLa-II** (right). All H atoms except those attached to water or phosphonate oxygen atoms are omitted for clarity. (c) Scheme of phase transition between **CoLa-II** and **CoLa-III**.

(Figure S1). As a result, the CoLa(notp)$(H_2O)_4$ layer in **CoLa-I** is more flat with the uncoordinated phosphonate oxygen atoms and coordinated water molecules protruding out toward the interlayer space (Figure 1b, left). These sites could then serve to anchor the lattice water molecules or directly transfer protons as part of a conduction pathway in the *ab* plane (Figure S3, left). For compound **CoLa-II**, the $[CoLa(notpH)(H_2O)_6]^+$ layer is more acidic because of the protonation of one phosphonate oxygen atom and also more twisted with the coordinated water molecules sitting in the middle of the layer (Figure 1b, right). The two sides of the layer are shielded by the organic groups of $notpH^{5-}$. The interlayer space is largely blocked by the hydrophobic organic groups as well as the large ClO_4^- anions. Hence the proton conduction pathway is efficient only along the *a*-axis, which is lined with the protonated phosphonate oxygen atoms, the coordinated and lattice water molecules as H-bond donors or acceptors (Figure S3, right).

Thermal analyses show that only 4.5 and 3.5 lattice water molecules remain in powder samples of **CoLa-I** and **CoLa-II**, respectively (Figure S4). Apparently, the lattice water molecules can be partially escaped under the ambient condition. In order to determine the stability of structures **CoLa-I** and **CoLa-II**, we keep the samples at different temperatures and humidities for 20 h. For **CoLa-I**, the PXRD patterns show that the diffraction peak at 6.3°, indexed as (002), moves to 7.3° for the powder sample of **CoLa-I** and also the samples kept at 25 °C and 40−80% RH for 20 h (Figure S6−S8), corresponding to a smaller interlayer distance (12.10 vs 14.02 Å in the single crystal). When the humidity is above 90%, two peaks appear at 6.3° and 7.3°, respectively, indicating that both **CoLa-I**(·8H_2O) and **CoLa-I**(·4.5H_2O) are present in the sample. Same phenomenon is observed for the samples kept at 93% RH and different temperatures (15−55 °C) (Figure S9).

In contrast, the PXRD patterns of **CoLa-II** remain almost the same at 25 °C and 40−93% RH (Figure S10). It means that the release of partial lattice water has little influence on the interlayer distance and also the cell parameters, possibly due to the presence of ClO_4^- anions in the interlayer space. When the temperature is increased to 45 °C (93% RH), however, a new phase **CoLa-III** is formed (Figure S11). Interestingly, its PXRD pattern is quite similar to that of **CoLa-I** (Figure 2), although

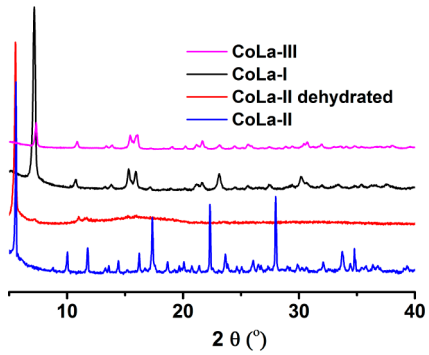

Figure 2. PXRD patterns of **CoLa** compounds and also the dehydrated sample of **CoLa-II** pretreated at 100 °C under vacuum for 2 h.

slight differences in peak positions are observed (Figure S6, Table S5). The energy dispersive X-ray spectroscopy (EDX) measurements reveal that the atomic ratios of La:Co:Cl are about 1:1:0 for **CoLa-I** and 1:1:1 for **CoLa-II** and **CoLa-III**, respectively (Figures S13−S14, Table S6). Apparently, the ClO_4^- anion remains in **CoLa-III**. The X-ray absorption fine structure (XAFS) spectroscopy can provide information about the local environment around the metal ions. Thus, we also investigate the XAFS measurements for the three samples (Figures S15−S20). The curve-fitting for the first FT peak in the R-space is conducted for the Co K-egde and La L3-edge EXAFS data (Figures S19−S20, Tables S7−10). For **CoLa-III**, the fitting results in three Co−N bonds at 1.92 Å, three Co−O bonds at 1.94 Å, and eight La−O bonds at 2.59 Å, which agrees well with those of **CoLa-I**. Based on the PXRD, EDX, and EXAFS results, it can be concluded that compound **CoLa-III** is isostructural to **CoLa-I** with the presence of ClO_4^- between the layers. The interlayer distance obtained from the PXRD data is 12.02 Å. Combining with the elemental and thermal analyses, we propose that the formulas of **CoLa-III** is (H_3O)[CoLa-(notp)$(H_2O)_4$]ClO_4·3H_2O. By immersing **CoLa-III** in water, the ClO_4^- anions can be removed completely as supported by the EDX measurements, leading to a complete transformation into **CoLa-I**.

Water absorption and desorption isotherms on samples **CoLa-I** and **CoLa-II**, pretreated at 100 °C under vacuum for 2 h, reveal that both experience similar one-step absorption processes in the P/P_0 range of 0−0.97 (Figure 3). However, the desorption isotherms show steps in both cases. For **CoLa-I**, the number of water molecules per molecular unit are 8.94, 5.77, and 4.24 at P/P_0 of 0.61, 0.19 and 0.02, respectively. The first one corresponds to four coordinated and 4.9 lattice water molecules, in agreement with the phase **CoLa-I**(·4.5H_2O) at 25 °C and 60% RH. When P/P_0 = 0.02, only four coordinated water remains, suggesting that all lattice water are removed. For

dx.doi.org/10.1021/ja505916c | *J. Am. Chem. Soc.* 2014, 136, 9292−9295

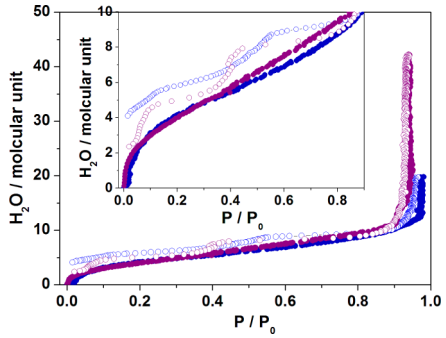

Figure 3. Water adsorption (filled circle) and desorption (open circle) isotherms of **CoLa-I** (blue) and **CoLa-II** (purple) at 25 °C. The inset is the same plot in the range of $0 \leq P/P_o \leq 0.9$.

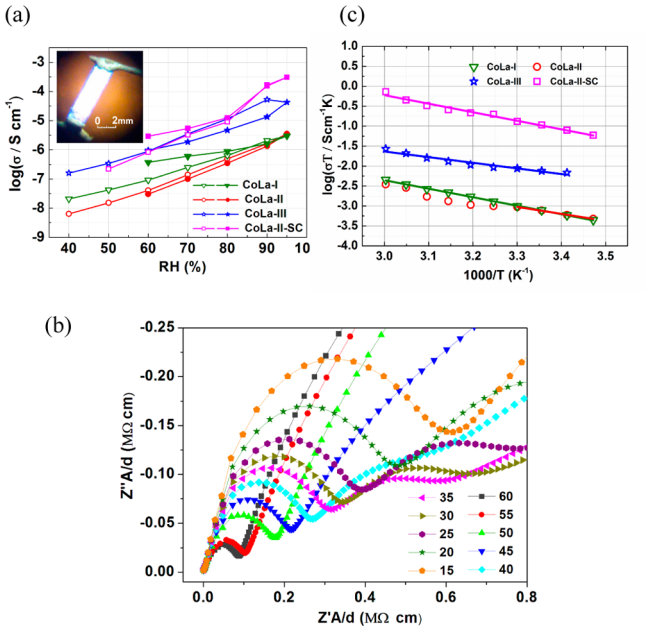

Figure 4. (a) Plots of log(σ) vs RH at 25 °C for **CoLa** compounds. The filled and open points correspond to the absorption and desorption processes, respectively. Inset: A view of gold wires connection on the sides of one single crystal of **CoLa-II**. (b) Nyquist plots for **CoLa-II** at 95% RH and various temperatures. (c) Plots of log(σT) vs 1000/T at 95% RH for **CoLa** compounds. The solid lines represent the best fit of the data.

CoLa-II, the water molecules per molecular unit are 8.14, 4.94, and 2.36 at P/P_0 of 0.53, 0.18 and 0.02, respectively. The latter two values are smaller than the number of coordination water in **CoLa-II**, indicating that even the coordination water can be released when the humidity is low enough (below 37%). The samples can be rehydrated. The PXRD patterns confirm that the dehydration/rehydration process for compound **CoLa-I** is reversible, while that for **CoLa-II** is not (Figure S21). Instead, the pattern of rehydrated **CoLa-II** is very similar to that of **CoLa-I**, although the framework structure of **CoLa-II** remains after dehydration. The results again demonstrate that a solid-state phase transition occurs for compound **CoLa-II** under humidity, forming a new phase of **CoLa-III** in which the layer structure is the same as that in **CoLa-I**. It means that the proton in the phosphonate group in **CoLa-II** has to be released into the interlayer space with the formation of hydronium ions in **CoLa-III**. Thus, an enhancement of proton conductivity is expected.

The proton conductivities of **CoLa-I**, **II**, and **III** are evaluated by ac impedance spectroscopy using a compacted pellet of the powder sample with two gold electrodes attached to the surface. At 25 °C and 95% RH, the proton conductivities are 3.00×10^{-6} and 3.50×10^{-6} S cm^{-1} for **CoLa-I** and **CoLa-II**, respectively. The values drop to 2.09×10^{-8} and 6.46×10^{-9} S cm^{-1} for the two samples at 25 °C and 40% RH (Figure 4a). The strong humidity dependence of conductivity suggests that the water molecules present in the interlayer spaces are important for the proton conduction. It is interesting to note that the proton conductivity of **CoLa-II** is similar to that of **CoLa-I**, although the layer of **CoLa-II** is more acidic than that of the latter. This result can be explained by the fact that the proton conductivity is efficient in the *ab* plane in compound **CoLa-I**, while only along the *a*-axis in compound **CoLa-II**. To justify this proposal, a single crystal measurement would be required. Fortunately a large single crystal of **CoLa-II** (**CoLa-II-SC**) is available, and the crystal face can be determined by X-ray diffraction (Figure S22). Two gold electrodes are attached to the two sides of the crystal along the *a*-axis (Figure 4a, inset). The proton conductivity is measured as 3.05×10^{-4} S cm^{-1} at 25 °C and 95% RH, which is much larger than that for the powder sample by 2 orders of magnitude (Figure 4a). It demonstrates that the direction of H-bond extension is the preferred proton conduction pathway in the crystal structure. For **CoLa-III**, the proton conductivity is 4.24×10^{-5} S cm^{-1} at 25 °C and 95% RH, 1 order of magnitude higher than those for **CoLa-I** and **CoLa-II**, indicating that the phase transition and the release of proton into the interlayer space can significantly enhance the proton conductivity of the material.

Temperature dependence of the conductivity is measured from 15 to 60 °C at 95% RH for all samples. The Nyquist plots for **CoLa-II** are shown in Figure 4b. The activation energies (E_a) are estimated to be 0.42, 0.42, and 0.28 eV for **CoLa-I**, **CoLa-II-SC**, and **CoLa-III**, respectively (Figure 4c). For **CoLa-II**, a linear dependence is found only in the range of 15−30 °C, above which a distinct deviation is observed. This deviation could be attributed to the phase transition of **CoLa-II** in the solid state. The activation energy is 0.34 eV for **CoLa-II** based on the data of 15−30 °C. For **CoLa-II-SC**, the deviation from linear dependence is not significant, indicating that the conductivity of **CoLa-II** along the *a*-axis remains similar before and after phase transition. All these values are low enough to assume that the conduction mechanism is of the Grotthuss fashion.[1b]

In summary, we report the proton conductivity of layered 3d−4f phosphonates. The results demonstrate that the phase transition in the solid state, accompanied by the release of proton from intralayer to interlayer space, can significantly enhance the proton conduction of the material. This work opens a new route in searching for high performance proton conductors.

■ ASSOCIATED CONTENT

Ⓢ Supporting Information

Synthetic details, experimental procedures, structural data, EDX, TG analyses, PXRD, IR, additional structural figures and Nyquist plots, and XAFS spectra. This material is available free of charge via the Internet at http://pubs.acs.org.

dx.doi.org/10.1021/ja505916c | J. Am. Chem. Soc. 2014, 136, 9292−9295

AUTHOR INFORMATION

Corresponding Author

lmzheng@nju.edu.cn; kitagawa@kuchem.kyoto-u.ac.jp

Notes

The authors declare no competing financial interest.

ACKNOWLEDGMENTS

This work is supported by the National Basic Research Program of China (2010CB923402, 2013CB922102) and the NSF of China (nos. 11079021, 21101092). This paper is dedicated to Prof. Xin-Quan Xin on the occasion of his 80th birthday.

REFERENCES

(1) (a) *Proton Conductors: Solids, Membranes and Gels-Materials and Devices*; Colomban, P., Ed.; Cambridge University Press: Cambridge, 1992; Vol. *2*, Chemistry of Solid State Materials. (b) Kreuer, K. D. *Chem. Mater.* **1996**, *8*, 610. (c) Kreuer, K. D.; Paddison, S. J.; Spohr, E.; Schuster, M. *Chem. Rev.* **2004**, *104*, 4637. (d) Alberti, G.; Casciola, M. *Solid State Ionics* **2001**, *145*, 3.

(2) (a) Yamada, T.; Otsubo, K.; Makiura, R.; Kitagawa, H. *Chem. Soc. Rev.* **2013**, *42*, 6655. (b) Yoon, M.; Suh, K.; Natarajan, S.; Kim, K. *Angew. Chem., Int. Ed.* **2013**, *52*, 2688. (c) Li, S.-L.; Xu, Q. *Energy Environ. Sci.* **2013**, *6*, 1656.

(3) (a) Kitagawa, H.; Nagao, Y.; Fujishima, M.; Ikeda, R.; Kanda, S. *Inorg. Chem. Commun.* **2003**, *6*, 346. (b) Yamada, T.; Sadakiyo, M.; Kitagawa, H. *J. Am. Chem. Soc.* **2009**, *131*, 3144. (c) Sadakiyo, M.; Yamada, T.; Kitagawa, H. *J. Am. Chem. Soc.* **2009**, *131*, 9906. (d) Sahoo, S. C.; Kundu, T.; Banerjee, R. *J. Am. Chem. Soc.* **2011**, *133*, 17950.

(4) (a) Hurd, J. A.; Vaidhyanathan, R.; Thangadurai, V.; Ratcliffe, C. I.; Moudrakovski, I. L.; Shimizu, G. K. H. *Nat. Chem.* **2009**, *1*, 705. (b) Bureekaew, S.; Horike, S.; Higuchi, M.; Mizuno, M.; Kawamura, T.; Tanaka, D.; Yanai, N.; Kitagawa, S. *Nat. Mater.* **2009**, *8*, 831. (c) Umeyama, D.; Horike, S.; Inukai, M.; Hijikata, Y.; Kitagawa, S. *Angew. Chem., Int. Ed.* **2011**, *50*, 11706. (d) Horike, S.; Umeyama, D.; Inukai, M.; Itakura, T.; Kitagawa, S. *J. Am. Chem. Soc.* **2012**, *134*, 7612. (e) Umeyama, D.; Horike, S.; Inukai, M.; Itakura, T.; Kitagawa, S. *J. Am. Chem. Soc.* **2012**, *134*, 12780.

(5) (a) Ohkoshi, S.-I.; Nakagawa, K.; Tomono, K.; Imoto, K.; Tsunobuchi, Y.; Tokoro, H. *J. Am. Chem. Soc.* **2010**, *132*, 6620. (b) Pardo, E.; Train, C.; Gontard, G.; Boubekeur, K.; Fabelo, O.; Liu, H.; Dkhil, B.; Lloret, F.; Nakagawa, K.; Tokoro, H.; Ohkoshi, S.-i.; Verdaguer, M. *J. Am. Chem. Soc.* **2011**, *133*, 15328.

(6) (a) Meng, X.; Song, X.-Z.; Song, S.-Y.; Yang, G.-C.; Zhu, M.; Hao, Z.-M.; Zhao, S.-N.; Zhang, H.-J. *Chem. Commun.* **2013**, *49*, 8483. (b) Dong, X.-Y.; Wang, R.; Li, J.-B.; Zang, S.-Q.; Hou, H.-W.; Mak, T. C. W. *Chem. Commun.* **2013**, *49*, 10590.

(7) (a) Shigematsu, A.; Yamada, T.; Kitagawa, H. *J. Am. Chem. Soc.* **2011**, *133*, 2034. (b) Sen, S.; Nair, N. N.; Yamada, T.; Kitagawa, H.; Bharadwaj, P. *J. Am. Chem. Soc.* **2012**, *134*, 19432.

(8) Taylor, J. M.; Dawson, K. W.; Shimizu, G. K. H. *J. Am. Chem. Soc.* **2013**, *135*, 1193.

(9) Sadakiyo, M.; Ōkawa, H.; Shigematsu, A.; Ohba, M.; Yamada, T.; Kitagawa, H. *J. Am. Chem. Soc.* **2012**, *134*, 5472.

(10) Jeong, N. C.; Samanta, B.; Lee, C. Y.; Farha, O. K.; Hupp, J. T. *J. Am. Chem. Soc.* **2012**, *134*, 51.

(11) (a) Grohol, D.; Subramanian, M. A.; Poojary, D. M.; Clearfield, A. *Inorg. Chem.* **1996**, *35*, 5264. (b) Taylor, J. M.; Mah, R. K.; Moudrakovski, I. L.; Ratcliffe, C. I.; Vaidhyanathan, R.; Shimizu, G. K. H. *J. Am. Chem. Soc.* **2010**, *132*, 14055. (c) Bazaga-García, M.; Colodrero, R. M. P.; Papadaki, M.; Garczarek, P.; Zoń, J.; Olivera-Pastor, P.; Losilla, E. R.; León-Reina, L.; Aranda, M. A. G.; Choquesillo-Lazarte, D.; Demadis, K. D.; Cabeza, A. *J. Am. Chem. Soc.* **2014**, *136*, 5731. (d) Liang, X.; Zhang, F.; Feng, W.; Zou, X.; Zhao, C.; Na, H.; Liu, C.; Sun, F.; Zhu, G. *Chem. Sci.* **2013**, *4*, 983. (e) Kim, S.-R.; Dawson, K. W.; Gelfand, B. S.; Taylor, J. M.; Shimizu, G. K. H. *J. Am. Chem. Soc.* **2013**, *135*, 963. (f) Taylor, J. M.; Dawson, K. W.; Shimizu, G. K. H. *J. Am. Chem. Soc.* **2013**, *135*, 1193.

(12) Bao, S.-S.; Liao, Y.; Su, Y.-H.; Liang, X.; Hu, F.-C.; Sun, Z.-H.; Zheng, L.-M.; Wei, S.-Q.; Alberto, R.; Li, Y.-Z.; Ma, J. *Angew. Chem., Int. Ed.* **2011**, *50*, 5504.

(13) Crystal data for **CoLa-II**: monoclinic, $P2_1/n$, a = 8.5537(10), b = 31.875(3), c = 13.6466(12) Å, β = 90.014(2)°, V = 2902.8(5) Å^3, Z = 4, $F(000)$ = 1816, ρ_{calcd} = 2.063 g cm^{-3}, μ (MoKα) = 2.382 mm^{-1} (λ = 0.71073 Å), R1 = 0.0349, wR2 = 0.0820, GooF = 1.00. CCDC 983043 contains the supplementary crystallographic data for this paper.